IOP Publishing New J. Phys. 24 (2022) 123006 https://doi.org/10.1088/1367-2630/aca556

New Journal of Physics
The open access journal at the forefront of physics

Deutsche Physikalische Gesellschaft DPG
IOP Institute of Physics

Published in partnership with: Deutsche Physikalische Gesellschaft and the Institute of Physics



OPEN ACCESS

RECEIVED
13 July 2022

REVISED
12 September 2022

ACCEPTED FOR PUBLICATION
23 November 2022

PUBLISHED
9 December 2022

Original Content from this work may be used under the terms of the Creative Commons Attribution 4.0 licence.

Any further distribution of this work must maintain attribution to the author(s) and the title of the work, journal citation and DOI.



PAPER

Emergent thermophoretic behavior in chemical reaction systems

Shiling Liang (梁师翎)[1], Daniel Maria Busiello[1,2] and Paolo De Los Rios[1,3,*]

[1] Institute of Physics, École Polytechnique Fédérale de Lausanne (EPFL), 1015 Lausanne, Switzerland
[2] Max Planck Institute for the Physics of Complex Systems, 01187 Dresden, Germany
[3] Institute of Bioengineering, École Polytechnique Fédérale de Lausanne (EPFL), 1015 Lausanne, Switzerland
[*] Author to whom any correspondence should be addressed.

E-mail: paolo.delosrios@epfl.ch

Keywords: thermophoresis, non-equilibrium thermodynamics, reaction–diffusion system, Soret effect, transport phenomena, thermodiffusion

Abstract

Exposing a solution to a temperature gradient can lead to the accumulation of particles on either the cold or warm side. This phenomenon is known as thermophoresis, and its microscopic origin is still debated. Here, we show that thermophoresis can be observed in any system having internal states with different transport properties, and temperature-modulated rates of transitions between the states. These internal degrees of freedom might be configurational, chemical or velocity states. We also derive an expression for the Soret coefficient, which decides whether particles accumulate on the cold or warm side. Our framework can be applied to any chemical reaction system diffusing in a temperature gradient. It also captures the possibility to observe a sign inversion of the Soret coefficient as the competition between chemical and velocity states. We establish thermophoresis as a genuine non-equilibrium effect, originating from internal microscopic currents consistent with the necessity of transporting heat from warm to cold regions.

1. Introduction

A solution in contact with a temperature gradient exhibits a phenomenon known as thermophoresis, thermodiffusion, or Ludwig–Soret effect [1, 2]. This is characterized by the migration of particles towards either the cold or warm side of the gradient, leading to a non-uniform stationary distribution [3]. The first evidence of thermophoresis dates back to the work of Ludwig in 1856 [4]. Since then, it has been observed in several different systems, such as colloidal suspensions [5], biomolecular solutions [6, 7], fluid mixtures [8] and DNA beads [9], just to cite some examples.

Despite the overwhelming experimental evidence, a comprehensive microscopic theory of thermophoresis is still lacking [10]. One of the main difficulties consists in the fact that most of the theoretical efforts rooted in system-dependent modeling have fallen short of determining the essential ingredients responsible for the emergence of thermophoresis [11]. Moreover, although thermophoresis feeds upon the imposed thermal gradient, the role of energy fluxes and their inevitable dissipation is a long-standing issue [12].

Heuristically, thermophoresis acts on the system as an external velocity drift, v_T. For diluted concentrations, it is usually assumed that v_T is proportional to the temperature gradient, i.e. $v_T = -D_T \partial_x T$, where D_T is the thermodiffusion coefficient [3, 13], assuming, for sake of simplicity, to have a one-dimensional system. The presence of this additional velocity leads to an extra concentration flux, $J_T = v_T c$, where c is the particle concentration. The contribution coming from this drift competes with the standard diffusive flux, $J_D = -D\partial_x c$, just as any other drift term would, resulting in a non-uniform distribution at steady state. Indeed, the stationary concentration of particles, c^{ss}, is determined by employing the zero-flux condition [14]:

$$\frac{\partial_x c^{ss}}{c^{ss}} = -S_T \partial_x T \tag{1}$$

© 2022 The Author(s). Published by IOP Publishing Ltd on behalf of the Institute of Physics and Deutsche Physikalische Gesellschaft

where $S_T = \frac{D_T}{D}$ is the so-called Soret coefficient, defined as the ratio between the thermodiffusion and the diffusion coefficients, which govern the two competing contributions to the total flux, J_T and J_D. Depending on the sign of S_T, the particles accumulate on the cold or warm side of the gradient.

Equation (1) is phenomenological, and it is not obtained from a microscopic theory. It is not known, for example, which are the system properties determining the sign of the Soret coefficient. Most importantly, it is still unclear how to reconcile the zero-flux condition used to derive equation (1) with the presence of a thermal gradient and its thermodynamic consequences, e.g. heat transport and energy fluxes. The fact that thermophoresis is a complex phenomenon with many contributions to the overall Soret coefficient is one of the key challenges in developing a comprehensive theory from a microscopic description [11, 15]. Indeed, to capture the origin of thermophoresis, one needs to pinpoint all possible contributions (e.g. chemical states, temperature-dependent diffusion, solute–solvent interactions) and determine the leading terms under different circumstances.

Here, we focus on the role of the internal states, whether they are structural or chemical, deriving a general framework that can be applied to any chemical reaction network. Starting from the description of reaction–diffusion systems, we provide a microscopic derivation of the phenomenological equation (1), and find an expression of the Soret coefficient as a function of the internal parameters. Furthermore, we show that the onset of thermophoresis is inextricably related to the presence of non-vanishing fluxes in the system. Our approach extends to single-state particles, highlighting that in this case, the role of internal states is played by different velocities in the complete underdamped description of the system. Finally, we put together the contributions from internal states and velocities in a paradigmatic chemical reaction system, showing that an inversion of the sign of the Soret coefficient is theoretically plausible in this scenario. A previously reported result [16, 17], built on the assumption of a close-to-equilibrium regime, is also properly discussed within our framework, by means of a thermodynamic energetic approach.

The proposed theory accounts for the contribution of internal states with different transport properties to the emergent thermophoretic behavior. The thermo-sensitive contribution to the Soret coefficient stemming from internal structural changes has been indeed investigated in several experimental and theoretical settings, including poly(*N*-isopropyl acrylamide) (PNIPAM) systems [18–20], DNA folding and RNA stem-loop [21], and monomer-micellar transition [22]. We remark that a quantitative understanding of these real systems requires a careful assessment of all possible chemical reactions, including complex solute-solvent interactions. However, the approach presented here highlights the role and interplay of crucial microscopic ingredients (e.g. reaction rates, diffusion coefficients, and energies), thus providing a qualitative grasp even on more complicated settings.

2. Thermophoresis in chemical space

We first consider a system composed of particles with multiple internal states in a solution, in the presence of a thermal gradient, $T(x)$. Despite being idealized, this model can be easily adapted to describe a large variety of systems, ranging from polymer chains to enantiomers, and catalytic enzymes. In the case of polymer chains, for which thermophoresis has been observed, internal states can be associated to different conformations [23]. Analogously, simple molecules can explore different isomers, each associated with an internal state, and enzymes can be bound to the substrate, the product or be unbound.

In what follows, we deal with linear reactions $X_i \rightleftharpoons X_j$, such as isomerization processes, even if it is straightforward to generalize the model to multi-molecular reactions (e.g. catalysis), as we will show later in this work. The probability of occupation of each internal state $i = 1, \dots n$ (e.g. chemical species), P_i, evolves according to Markovian dynamics and follows a reaction–diffusion equation [24]:

$$\partial_t P_i = D_i \partial_x^2 P_i + \sum_{j=1}^{n} k_{ij} P_j, \tag{2}$$

where k_{ij} is the rate at which state j transforms into state i, with the usual relation $k_{ii} = -\sum_{j(\neq i)} k_{ji}$ to ensure probability conservation, and D_i is the diffusion coefficient of state i. The transition rates satisfy the local detailed balance, $k_{ij}/k_{ji} = e^{-(E_i - E_j)/k_B T(x)}$, so that the local stationary solution due to the reaction part only coincides with the Boltzmann distribution at temperature $T(x)$. In this formulation, temperature enters implicitly in the kinetic rates, for which we do not provide yet an explicit expression. As a first approximation, we are considering diffusion coefficients that do not depend on temperature, in order to show that thermophoresis can emerge even in this simple setting. Thus, the resulting Soret coefficient is named *chemical* Soret coefficient, S_T^{ch}, to stress that it only accounts for the temperature modulation of chemical interactions. Summing over the internal states, we obtain the spatial probability distribution of particles, $P_{tot}(x) = \sum_i P_i(x)$, which is the quantity usually measured when studying thermophoresis.

2.1. A simple example: 2-state case

In the simplest case of only two internal states, equation (2) can be fully solved. Employing the zero-flux condition only on P^{ss}_{tot} at stationarity, hence allowing for the existence of fluxes in the internal space (e.g. among chemical states), we find [14]:

$$\partial_x \left(\left(\langle D \rangle_{eq} P^{ss}_{tot} \right) - \left(\frac{D_1 D_2}{k_{sum}} \partial_x^2 P^{ss}_{tot} \right) \right) = 0 \tag{3}$$

where $k_{sum} = k_{12} + k_{21}$, and $\langle D \rangle_{eq} = (D_1 k_{12} + D_2 k_{21})/k_{sum}$, the equilibrium ensemble average diffusion coefficient. For slowly varying functions (small wavelength approximation, i.e. $\partial_x^2 P^{ss}_{tot} \simeq 0$), and/or for chemical reactions much faster than diffusion, equation (3) takes the same form as equation (1), with the identification

$$\frac{\partial_x P^{ss}_{tot}}{P^{ss}_{tot}} = -S^{ch}_T \partial_x T \qquad \rightarrow \qquad S^{ch}_T = \frac{\partial_T \langle D \rangle_{eq}}{\langle D \rangle_{eq}}. \tag{4}$$

We remark that we started from a complete description of a reaction–diffusion system in terms of occupation probabilities. However, the resulting equation (4) exhibits the same phenomenology as the customary description of thermophoresis in equation (1). It is thus natural to identify an effective Soret coefficient, S^{ch}_T, in terms of an effective diffusion coefficient, $\langle D \rangle_{eq}$. The spatial and temperature dependence in $\langle D \rangle_{eq}$ results from an averaging procedure over internal states and is not a consequence of the temperature dependence of the single diffusion coefficients, D_i. Hence, $\langle D \rangle_{eq}$ depends on x and $T(x)$ through the kinetic rates k_{ij}. This result immediately reveals that a necessary condition for thermophoresis (i.e. a non-uniform P^{ss}_{tot}) is that $D_1 \neq D_2$.

We show in [14] that any two-state system can be represented with coupled diffusion equations not obeying local continuity equation in the space of P_{tot} and $\Pi = P_1 - P_2$. At equilibrium, i.e. $\Delta T = 0$, the source/sink additional terms will vanish. In non-equilibrium condition they do not, thus indicating that the system is supporting non-equilibrium fluxes that are deceptively *hidden* in the customary, zero-flux, phenomenological description of equation (1). These fluxes are actually a thermodynamic necessity for heat transport from warm to cold regions. Within the small wavelength approximation, the heat flux across the system is [14]:

$$\frac{J_E}{-\partial_x T} = D_1 D_2 \frac{E_1 - E_2}{D_1 - D_2} S^{ch}_T P^{ss}_{tot} > 0 \tag{5}$$

which is directed from the warm to the cold side. Equation (5) quantifies the energy flux originating from the transition among the internal states (two in this case). Indeed, when $E_1 = E_2$ they can be merged into a single moiety and only the heat flux due to the solvent, which is not explicit in this framework, survives. Thermophoresis, particle fluxes, and thermodynamically necessary heat fluxes are inextricably intertwined.

2.2. Fast-reaction limit

The expression for the Soret coefficient in equation (4) can be obtained for a general reaction network obeying equation (2), by employing the fast-reaction limit. In this approximation, which is equivalent to the small wavelength approximation, the transition rates between chemical states, k_{ij}, are much faster than diffusion, a realistic condition in many experimental settings [25, 26], and the system locally relaxes to equilibrium. With further developments, when k_{ij} takes the usual Arrhenius form for temperature-activated transitions [14]:

$$S^{ch}_T = \frac{\partial_T \langle D \rangle_{eq}}{\langle D \rangle_{eq}} = \frac{\langle ED \rangle_{eq} - \langle E \rangle \langle D \rangle_{eq}}{\langle D \rangle_{eq} k_B T^2} = \frac{\mathbf{Cov}_{eq}(E, D)}{\langle D \rangle_{eq} k_B T^2}. \tag{6}$$

Again, this expression is derived from a description in terms of reaction rates and (constant) diffusion coefficients. As before, $\langle D \rangle_{eq}$ is an effective diffusion coefficient that depends on space only through k_{ij}. This result provides an insight into the physical origin of the Soret coefficient and into its intimate structure. It highlights the intrinsic relation between thermophoresis and how energies and diffusion coefficients are distributed among the internal states. In particular, when high-energy states diffuse faster, particles tend to accumulate on the cold side, and vice versa. This observation might stimulate a new avenue of research about the possibility to design and control the thermophoretic response of bio-inspired chemical nanodevices [27, 28].

In figure 1, we report the steady-state profile, P^{ss}_{tot}, for a discrete-state system obeying equation (2). The fast-reaction limit provides an analytical limiting expression for S^{ch}_T, but thermophoresis can be observed

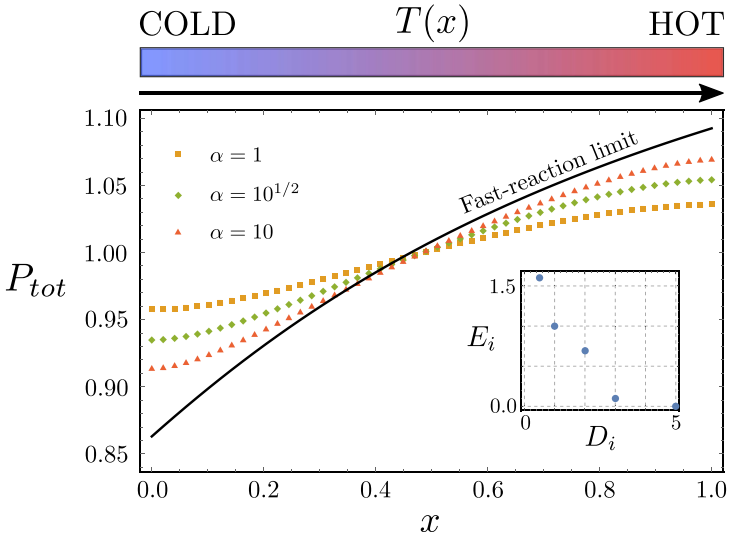


Figure 1. Steady-state distributions when $\mathbf{Cov}_{\rm eq}(E, D) < 0$ for different velocities of the Arrhenius transition rates: $k_{ij} = \alpha e^{(E_j - B_{ij})/k_{\rm B}T(x)}$, with $k_{\rm B}T(x) = 0.5 + x$ and B_{ij} energy barrier between states i and j. The solid line indicates the fast-reaction limit. Particles accumulate on the warm side, denoting a negative Soret coefficient. The inset shows energies and diffusion coefficients of all states. Parameters are reported in [14].

even away from this limit, provided that the diffusion coefficients of the internal (e.g. chemical) states are different.

We remark that our results can be extended to the case of a continuous chemical state-space, characterized by a potential energy function $U(\vec{q})$. In the discrete-state approximation, each deep minima of this functional identifies an internal state. Both equation (6) and the emergence of thermophoresis, as in figure 1, have their exact parallel in this more general setting [14].

3. Thermophoresis in phase-space

In the previous models, the diffusion constant was independent from space to highlight that thermophoresis emerges from the interplay between currents in real and internal space. Of course, if temperature depends on space, then, according to Einstein relation $D(x) = k_{\rm B}T(x)/\gamma$ (γ being the Stokes' friction coefficient) also the diffusion constant depends on x. Actually, this property alone is enough to induce an accumulation of particles on the cold side (as if in the presence of a positive Soret coefficient). In this case, we name $S_{\rm T}^0$ the corresponding Soret coefficient, to highlight that it is associated with particles with no internal states. In fact, we start from the Kramers equation for the evolution of $P(x, v, t)$ in the full phase-space:

$$\partial_t P + v\partial_x P = \frac{\gamma}{m}\partial_v \left(vP + \frac{k_{\rm B}T(x)}{m}\partial_v P \right) \tag{7}$$

where m is the particle mass. We show in [14] that the correct parameter to perform the overdamped limit is the friction characteristic time-scale $\tau = m/\gamma$. Hence, when $\tau^{-1} \ll 1$, the relaxation due to the friction is much faster than all other time-scales in play, i.e. the system experiences a faster equilibration in velocity space. As already derived in [29, 30], the marginal distribution in the x space, $\mathcal{P}(x)$, obtained by integrating over the fast variable v satisfies [14]:

$$\partial_t \mathcal{P}(x) = \frac{m}{\gamma}\partial_x^2 \left(\langle v^2 \rangle_{\rm eq} \mathcal{P}(x) \right). \tag{8}$$

Notice this expression has no ambiguity on how to include the spatial dependency of the diffusion coefficient [31]. Indeed, as discussed in [32, 33], the fast relaxation of velocities in the presence of a white noise, always gives equation (8) in the overdamped limit. Solving for the steady-state by employing the zero-flux condition, we obtain:

$$S_{\rm T}^0 = \frac{\partial_T \left(\langle v^2 \rangle_{\rm eq} \right)}{\langle v^2 \rangle_{\rm eq}} = \frac{1}{T(x)} \tag{9}$$

where $\langle \cdot \rangle_{\rm eq} = Z_{\rm eq}^{-1} \int {\rm d}v \cdot e^{-mv^2/(2k_{\rm B}T(x))}$ is the ensemble average over the equilibrium distribution in velocity space, and $Z_{\rm eq}$ the normalization factor. The $1/T$ form of the Soret coefficient can be regarded as a direct

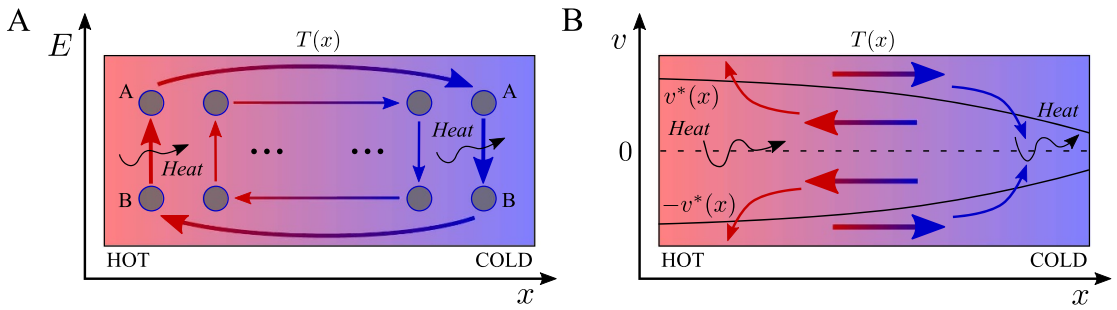


Figure 2. (A) - Heat is absorbed on the warm side, hence driving the system towards high-energy states. Afterwards, diffusion moves particles to the cold side, cooling them down and ending up populating low energy states. Eventually, the cycle restarts. (B) - As for panel (A), heat is absorbed on the warm side, and released on the cold side. When heated, particles overcome $v^*(x)$ and start moving towards the cold side. When cooled, they are driven below $v^*(x)$. In the full phase-space, there are two identical cycles above and below the zero-velocity line, since energy depends on $|v|$.

consequence of the Stokes–Einstein relation $D(x) = k_B T(x)/\gamma$. Indeed, the same dependence also emerges naturally in the ideal gas model, so that it is also referred to as ideal gas contribution [34].

This is clearly an oversimplified model, whose aim is only to show that the Soret coefficient stems, again, from the presence of internal states with different energies and different transport coefficients. In this case, the internal state variable is the velocity, and the internal state energy is the kinetic energy. Clearly, higher kinetic energy positively correlates with faster transport, resulting in a positive Soret coefficient (equation (9)).

3.1. Fluxes in phase-space

In the simple case of two internal states, although the total concentration was flux-less, there were spatial fluxes of the two states that, by conservation of the probability, are accompanied by fluxes in the internal space (figure 2, left panel). Analogously, when dealing with the case of underdamped single-state particles, non-equilibrium fluxes take place in the whole phase space, although they do not appear in the overdamped dynamical description. Their presence, however, is crucial both to sustain a non-uniform stationary marginalized distribution $\mathcal{P}(x)$, which is a signature of the presence of a thermophoretic effect, and to transport heat as dictated by the laws of thermodynamics.

The component of the current in position-space is $J_x(x, v, t) = vP(x, v, t)$ [14]. Its integral over the velocity space is zero because of the zero-flux condition in space. However, $J_x(x, v, t)$ is not zero in the whole phase-space (x, v), consistently with the non-equilibrium conditions. Indeed, the probability current of particles slower than $|v|$, for any $|v|$, is always parallel to $\partial_x T$ (thus directed from the cold to the warm side), implying that, because of the no-flux condition, the current accounting for particles faster than $|v|$, is always parallel to $-\partial_x T$. Both of them vanish only for $|v| = 0$ and $|v| \to +\infty$, reaching their maximum absolute value at $v^* = \sqrt{3T(x)/m}$.

Just as in the two-states case currents close in the internal space, here they close in velocity space, with slow particles *warming up* on the warm side and fast particles *cooling down* on the cold side (figure 2, right panel). The system thus picks up heat on the warm side, transports it across the system and releases it on the cold side. A detailed analysis of the total energy current in position space shows that, to the leading order, at stationarity:

$$J_x^E = \int_{-\infty}^{\infty} \frac{mv^2}{2} J_x \mathrm{d}v = -\frac{k_B}{2\mathcal{N}} \partial_x T \tag{10}$$

where $\mathcal{N}$ is the normalization factor of the steady-state solution [14]. Equation (10) is reminiscent of Fourier's law for heat conduction in gases.

4. Thermophoresis in chemical reaction systems

In the previous sections, we derived two contributions to thermophoresis stemming from different internal degrees of freedom. The first one, S_T^{ch}, is associated with fluxes in the chemical space and a temperature-independent diffusion. Conversely, S_T^0 originates from the presence of particles with different velocities and the Stokes–Einstein relation. Including both these ingredients, i.e. an effective temperature-dependent diffusion for each internal state $D_i(T)$, the total phenomenological Soret coefficient, S_T, takes an additive form:

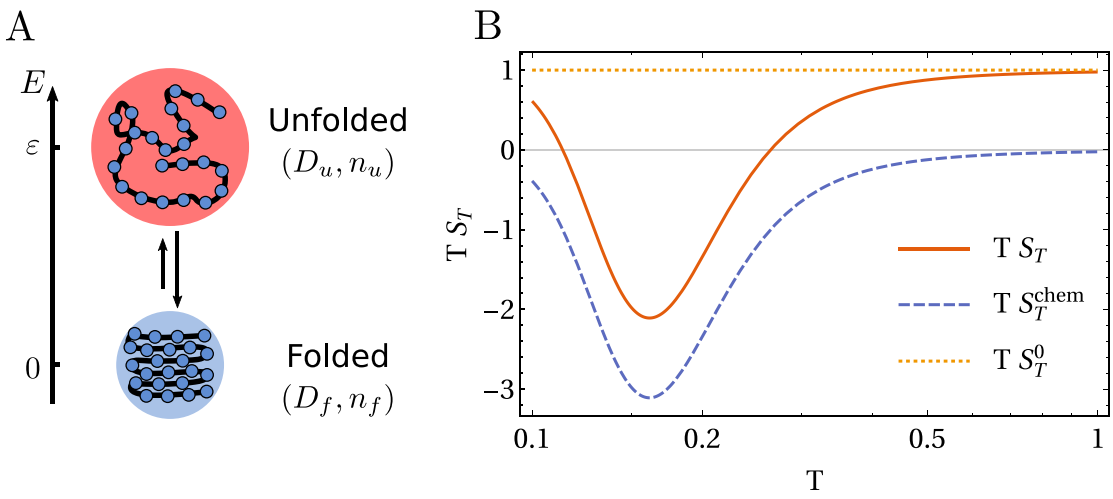


Figure 3. (A) - Isomerization reaction between the folded and unfolded states of a polymer. Due to the larger molecular size, the high-energy unfolded state has a larger diffusion coefficient than the folded state. The two degeneracy factors, n_u and n_f, account for the number of micro-states corresponding to these macro-states. (B) - The Soret coefficient of such a polymer has both the chemical and the ideal gas contribution, $S_{\rm T} = S_{\rm T}^{\rm ch} + S_{\rm T}^0$. The competition between these two terms allows for a sign inversion of $S_{\rm T}$ at different temperatures.

$$S_{\rm T} = S_{\rm T}^0 + S_{\rm T}^{\rm ch}. \tag{11}$$

In the appendix [14], we show how this structure emerges.

4.1. Sign inversion of $S_{\rm T}$ for polymers

Sign inversion of the Soret coefficient due to change of temperature has been observed in many systems [5, 35, 36]. An empirical relation, $S_{\rm T} = S_{\rm T}^{\infty}(1 - e^{(T-T^*)/T_0})$, has been proposed to describe this switching behavior, where T^* is the inversion temperature, and T_0 a scaling factor [5]. Here, we show that the sign inversion can emerge from the competition between the two contributions in equation (11), $S_{\rm T}^0$ and $S_{\rm T}^{\rm ch}$.

Let us consider a polymer with a folded (f) and an unfolded (u) macro-states, where the transitions between these two are triggered by thermal fluctuations. The folded state has lower energy and a more compact shape, thus diffusing faster than the unfolded one, $D_u < D_f$. Moreover, each macro-state is associated with several micro-states, n_u and n_f for unfolded and folded states, respectively. Including the entropic factors, the local detailed balance changes as follows: $k_{f\to u}/k_{u\to f} = \gamma\, e^{-\varepsilon/k_{\rm B}T}$, with $\gamma = n_u/n_f$, and ε the energy gap. Due to the energy-diffusion relation, the covariance in equation (6) is negative, leading to a negative Soret coefficient. Together with the ideal gas term, $S_{\rm T}^0$, the total Soret coefficient reads [14]:

$$S_{\rm T} = \underbrace{\frac{(R_d - 1)e^{\epsilon}\gamma\epsilon}{(e^{\epsilon} + \gamma)(e^{\epsilon} + R_d\gamma)}\frac{1}{T}}_{S_{\rm T}^{\rm ch}} + \underbrace{\frac{1}{T}}_{S_{\rm T}^0}, \tag{12}$$

where $R_d = D_u/D_f < 1$ and $\epsilon = \varepsilon/k_{\rm B}T$ is the rescaled energy gap. The two contributions have different signs, with $S_{\rm T}^{\rm ch}$ dominating only in a definite temperature range. In figure 3, we show that this setting allows for a sign inversion both from positive to negative and vice-versa, as reported by the a-dimensional quantity $TS_{\rm T}$ as a function of temperature.

This simple analysis of the competition between different thermophoretic contributions provides a possible mechanism for sign reversion. Although in biological systems there could exist more contributions to $S_{\rm T}$ [15, 34], our results hold for general chemical reaction networks in a temperature gradient. Moreover, the idea that internal states play a dominant role might be extended to different scenarios to understand other emergent thermophoresis-like behaviors.

It is worth noting that previous studies on PNIPAM systems have revealed a connection between an abrupt change in the particles' size and their thermal diffusion properties [18, 19]. In particular, the transition from a good to a bad solvent induces a collapse of PNIPAM chains from the coil to globular state. The peak of the Soret coefficient has been found at this transition point, consistently with the behavior of $\partial_T D$, where D is the measured diffusion coefficient [18]. This observation suggests a link between the transport properties of the internal states and the thermophoretic behavior analogous to the one predicted by our approach. In fact, the chemical Soret coefficient obtained using $\langle D\rangle_{\rm eq} \equiv D$ in equation (4)

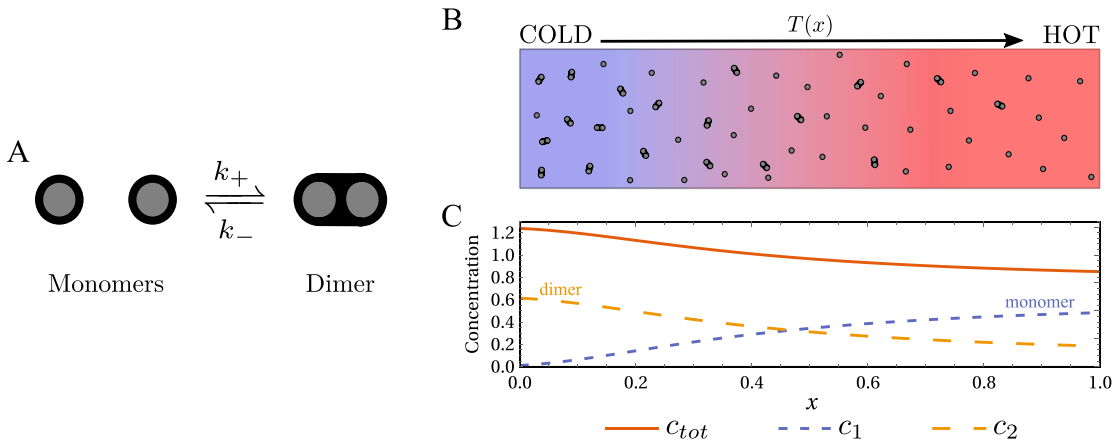


Figure 4. (A) - Schematic reaction scheme of dimer formation. (B) - Pictorial qualitative representation of dimer and monomer stationary populations in a thermal gradient. (C) - Steady-state theoretical profiles of dimer, monomer, and total concentration are shown in the fast reaction limit. The system supports the onset of thermophoresis.

qualitatively matches the experimental observation, even if our theory is not able to capture the strong solute–solvent interactions taking place in PNIPAM chains.

5. Thermophoresis and dimer formation

As an extension to the presented model, consider the case of non-dilute solutions in which interactions among particles are not negligible. This picture allows for the formation of complex states. In the simple case of dimer formation, the system is described by:

$$\begin{aligned}\partial_t c_1 &= 2k_- c_2 - 2k_+ c_1^2 + D_1 \partial_x^2 c_1 \\ \partial_t c_2 &= k_+ c_1^2 - k_- c_2 + D_2 \partial_x^2 c_2\end{aligned} \tag{13}$$

where c_1 and c_2 are, respectively, monomer and dimer concentrations, satisfying the normalization condition $c_1 + 2c_2 = c_{\rm tot}$, with $c_{\rm tot}$ total concentration. The dissociation constant has the usual form $K_d(x) = \frac{k_-(x)}{k_+(x)}$, where both association and dissociation rates depend on space through temperature.

Defining $\langle\cdot\rangle_{\rm eq} = \frac{1}{c_{\rm tot}} \sum_{n=1}^{2} \cdot\, n c_n^{\rm eq}$, the chemical Soret coefficient in the fast reaction limit is again of the form equation (6), and in particular [14]:

$$S_{\rm T}^{\rm ch} = -\frac{F(T, K_d, c_{\rm tot})}{1 - K_d F(T, K_d, c_{\rm tot})} \partial_T K_d \tag{14}$$

where we introduced the function $F(T, K_d, c_{\rm tot}) = \langle D \rangle_{\rm eq}^{-1} (D_1 - D_2) c_{\rm tot} K_d^{-2} g(T, K_d, c_{\rm tot})$, with $g(T, K_d, c_{\rm tot})$ always positive. Since dimers are typically larger than monomers, $D_1 - D_2 > 0$, and K_d increases with temperature (dimers tend to dissociate at higher temperatures), the Soret coefficient can be either negative or positive, with the overall concentration of molecules higher on the warm or cold side, respectively. While an accumulation on the cold side intuitively follows the direction of the heat flow, it is also possible to conceive complex scenarios, whereby dimers are stabilized by contacts between unstructured regions, as some in proteins, hence increasing temperatures might stabilize the dimer state.

In equation (9), we showed that single-state particles exhibit a positive Soret coefficient in dilute solutions. When particle-particle interactions become non-negligible, in non-dilute solutions, the potential formation of complex molecules may lead to an additional contribution to the Soret coefficient. The combination of these two effects might even result in an inversion of the thermophoretic response, as a function of particle concentrations, analogously to what we show above for a polymer.

In figure 4, we simulate the system of equation (13), showing the appearance of thermophoresis.

6. Discussion

We can establish a few, important, facts about thermophoresis:

- Thermophoresis emerges through the interplay between transport in real space and temperature-modulated transitions in some *internal* space, which can be a chemical, conformational, or velocity space

- The phenomenological approach to thermophoresis, equation (1), is an approximation of the correct equations, valid only in the fast reaction limit, and corresponding to the local-equilibrium assumption
- Equation (1) is customarily solved with the no-flux condition, hiding the presence of currents for the underlying degrees of freedom, which are present both in real and internal spaces. These currents are consistent with the non-equilibrium setting determined by the thermal gradient, and are actually a necessity for heat transport from warm to cold regions, as dictated by thermodynamics
- The Soret coefficient is related to the microscopic features of the system through the correlation between transport properties of each internal state and their energy. The proposed formula rationalizes the dependence on a multitude of system-specific factors, and provides the mathematical framework through which microscopic details must be assembled

A previous thermodynamic derivation of the Soret coefficient proposed by Braun and co-workers in [16, 17] argued that $S_T = T^{-1}\partial_T G$, where G is the free energy. To define a free energy, each point in space should be in equilibrium with a bath at the local temperature $T(x)$. This approach can be linked to the proposed framework by noting that, from stochastic thermodynamics arguments, $\mathrm{d}G = \mathrm{d}Q - T\mathrm{d}S$, Q being the heat and S the entropy. Furthermore, $\mathrm{d}Q = 0$ and $\mathrm{d}S = \mathrm{d}(-\log P_{\mathrm{tot}})$, since thermophoresis is captured by a description in terms of P_{tot}, which follows a purely diffusive equation under local-equilibrium assumptions. Hence, $S_T = \partial_T S = -\partial_T P_{\mathrm{tot}}/P_{\mathrm{tot}}$, being indeed proportional to a quantity encoding, through the derivative, information about spatial transport due to thermal gradients.

Our approach can be straightforwardly extended to several other systems with internal states. Along this line, a fascinating perspective of the proposed framework resides in the possibility of designing, in principle, an n-state system whose stationary concentration profile satisfies a target spatial shape, by tuning D_i and E_i suitably. Moreover, simple chemical systems could be experimentally tested, in order to verify and improve the theoretical grasp on the relationship between non-equilibrium fluxes, microscopic parameters, and thermophoresis. We expect that the contributions from internal states, captured by the presented theory, might be relevant when internal (e.g. structural) modifications induce abrupt changes in the diffusion coefficient as a function of the temperature, as it happens in PNIPAM systems. However, to provide a quantitative description of real systems already experimentally studied or more complex settings, e.g. with strong solute–solvent interactions, our framework have to be formulated so to consistently include some of the possible additional effects. We leave this task for future investigations.

Data availability statement

All data that support the findings of this study are included within the article (and any supplementary files).

Acknowledgment

We acknowledge F Piazza and R Livi for useful discussions and inspiring comments. S L and P D L R thank the Swiss National Science Foundation for support under Grant 200020_178763.

Appendix A. Simple example: two internal states

A.1. The exact stationary solution

To find the exact solution of a two-state diffusion-reaction system, let us define two variables: the sum $P_{\mathrm{tot}} = P_1 + P_2$ and the difference $\Pi = P_1 - P_2$. Using these two, we rewrite the time evolution equation:

$$\begin{aligned}\partial_t P_{\mathrm{tot}} &= \frac{D_1 + D_2}{2}\partial_x^2 P_{\mathrm{tot}} + \frac{D_1 - D_2}{2}\partial_x^2 \Pi \\ \partial_t \Pi &= \frac{D_1 - D_2}{2}\partial_x^2 P_{\mathrm{tot}} + \frac{D_1 + D_2}{2}\partial_x^2 \Pi + (k_{12} - k_{21})P_{\mathrm{tot}} - (k_{12} + k_{21})\Pi\end{aligned}. \tag{A.1}$$

Moving in Fourier space, we introduce the Fourier transform of each function:

$$\mathcal{F}(\Pi(x,t)) = \tilde{\Pi}(k,t) \quad \mathcal{F}(P_{\mathrm{tot}}(x,t)) = \tilde{P}_{\mathrm{tot}}(k,t) \tag{A.2}$$

hence, naming $\mathcal{D} = D_1 + D_2$ and $\Delta = D_1 - D_2$, we have the following set of equations:

$$\begin{aligned}&2\partial_t \tilde{P}_{\mathrm{tot}} + \mathcal{D}k^2 \tilde{P}_{\mathrm{tot}} + \Delta k^2 \tilde{\Pi} = 0 \\ &2\partial_t \tilde{\Pi} + \Delta k^2 \tilde{P}_{\mathrm{tot}} + \mathcal{D}k^2 \tilde{\Pi} - 2\mathcal{F}\left[(k_{12} - k_{21})P_{\mathrm{tot}}\right] + 2\mathcal{F}\left[(k_{12} + k_{21})\Pi\right] = 0.\end{aligned} \tag{A.3}$$

Solving the first equation, when $k \neq 0$, we have:

$$\tilde{\Pi}(k,t) = -\frac{2\partial_t \tilde{P}_{\rm tot}(k,t) + \mathcal{D}k^2 \tilde{P}_{\rm tot}(k,t)}{\Delta k^2} \tag{A.4}$$

that, in real space, corresponds to:

$$\Pi(x,t) = -\frac{\mathcal{D}}{\Delta} P_{\rm tot}(x,t) + \frac{2}{\Delta}\partial_t \left(\int_{-\infty}^{+\infty} d\xi \; P_{\rm tot}(\xi)(x-\xi)\text{sign}(x-\xi) \right). \tag{A.5}$$

A non-local term appears, which is the propagator of the one-dimensional Laplacian operator. It governs the diffusive dynamics of the system toward stationarity. However, the general solution of Π has to include an additional term:

$$\Pi(x,t) = -\frac{\mathcal{D}}{\Delta} P_{\rm tot}(x,t) + \frac{2}{\Delta}\partial_t \left(\int_{-\infty}^{+\infty} d\xi \; P_{\rm tot}(\xi)(x-\xi)\text{sign}(x-\xi) \right) + f(x) \tag{A.6}$$

where $f(x)$ is such that $\partial_x^2 f(x) = 0$. Inserting equation (A.6) into the second line of equation (A.1), multiplying by Δ, and dividing by $k_{\rm sum} = k_{12} + k_{21}$, we obtain:

$$\begin{aligned} &-\frac{D_1 + D_2}{k_{\rm sum}}\partial_t P_{\rm tot} - \left(D_1 \frac{k_{12}}{k_{\rm sum}} + D_2 \frac{k_{21}}{k_{\rm sum}} \right) P_{\rm tot} + \partial_t \left(\int \mathrm{d}\xi \; P_{\rm tot}(\xi,t)(x-\xi)\text{sign}(x-\xi) \right) \\ &+ \frac{1}{k_{\rm sum}}\partial_t^2 \left(\int \mathrm{d}\xi \; P_{\rm tot}(\xi,t)(x-\xi)\text{sign}(x-\xi) \right) + \frac{D_1 D_2}{k_{\rm sum}}\partial_x^2 P_{\rm tot} + (D_1 - D_2) f(x) = 0. \end{aligned} \tag{A.7}$$

This equation is directly in real space. We remark that we have divided by $k_{\rm sum}$, in order to isolate the term $f(x)$. Since we also know that the second spatial derivative of this function has to vanish, we can derive twice with respect to x:

$$\begin{aligned} &\partial_t P_{\rm tot} - \partial_x^2 \left(\left(D_1 \frac{k_{12}}{k_{\rm sum}} + D_2 \frac{k_{21}}{k_{\rm sum}} \right) P_{\rm tot} \right) \\ &\quad + \partial_x^2 \left(\frac{1}{k_{\rm sum}} D_1 D_2 \partial_x^2 P_{\rm tot} \right) \\ &- (D_1 + D_2)\partial_x^2 \left(\frac{1}{k_{\rm sum}} \partial_t P_{\rm tot} \right) + \partial_x^2 \left(\frac{1}{k_{\rm sum}} \partial_t^2 \int \mathrm{d}\xi \; P_{\rm tot}(\xi,t)(x-\xi)\text{sign}(x-\xi) \right) = 0. \end{aligned} \tag{A.8}$$

This form constitutes the exact solution, without any approximation. The first line is the same equation that appears in the fast reaction limit, derived in detail in the next section. The second line is the correction to compute the steady state, $P_{\rm tot}^{\rm ss}$, when the chemical reactions are not faster than diffusion. The last line controls the evolution of $P_{\rm tot}$ towards the steady state, and it contains the kernel of long-range interactions. At this point, we note that the fast reaction limit is, in general, a good approximation, since the only correction, at stationarity, is a fourth-order spatial derivative of $P_{\rm tot}^{\rm ss}$. In figure A1 we compare the steady-state profile in the fast reaction limit with two choices of parameters, $D_1 = 10^{-2}$ (reactions faster than diffusion), and $D_1 = 10^{-4}$ (reactions slower than diffusion).

For slowly varying functions, i.e. in the small wavelength approximation, corresponding to $\partial_x^2 P_{\rm tot}^{\rm ss} \simeq 0$, equation (A.8) takes the following form at stationarity:

$$\partial_x^2 \left(\left(D_1 \frac{k_{12}}{k_{\rm sum}} + D_2 \frac{k_{21}}{k_{\rm sum}} \right) P_{\rm tot}^{\rm ss} \right) = 0. \tag{A.9}$$

If the transition rates are of the usual Arrhenius-like form:

$$\frac{k_{21}}{k_{12}} = e^{(E_1 - E_2)/k_{\rm B}T(x)} \tag{A.10}$$

where E_i is the free energy of the state i, we define the equilibrium ensemble average of the diffusion coefficient:

$$\langle D \rangle_{\rm eq} = \frac{1}{Z^{\rm eq}} \sum_i D_i e^{-E_i/k_{\rm B}T(x)} \tag{A.11}$$

with $Z^{\rm eq}$ the equilibrium partition function.

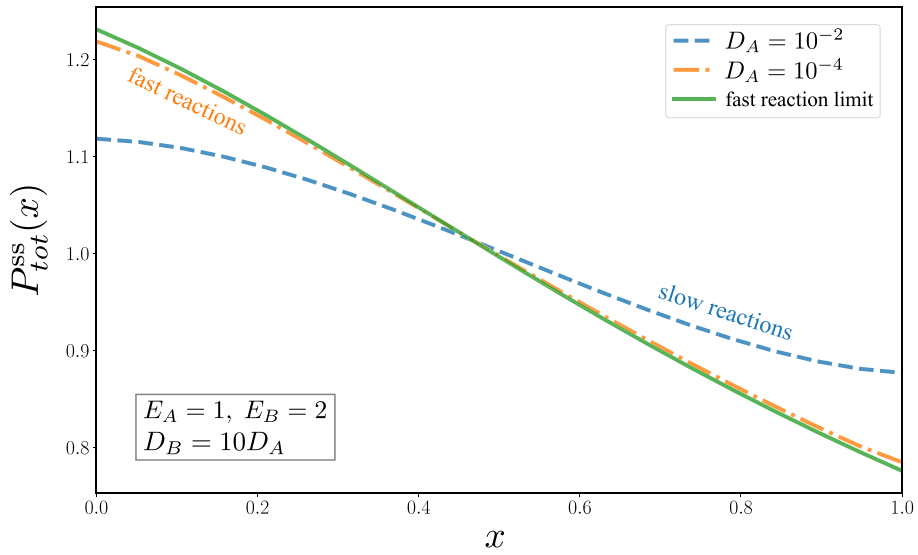


Figure A1. The steady-state profile of total probability $P^{ss}_{tot} = P^{ss}_A + P^{ss}_B$ is compared with two different choices of parameters: $D_1 = 10^{-2}$, for which reactions are slower than diffusion, and $D_2 = 10^{-4}$, for which reactions are faster than diffusion. The temperature gradient is set to $T(x) = 0.2(1 + x)$, for $x \in [0, 1]$.

Then, employing the zero-flux condition, we have the following equation for the stationary state:

$$P^{ss}_{tot}\partial_x\langle D\rangle_{eq} + \langle D\rangle_{eq}\partial_x P^{ss}_{tot} = 0 \tag{A.12}$$

which leads to the following identification of the (chemical) Soret coefficient:

$$\frac{\partial_x P^{ss}_{tot}}{P^{ss}_{tot}} = -\frac{\partial_T\langle D\rangle_{eq}}{\langle D\rangle_{eq}}\partial_x T. \tag{A.13}$$

A.2. The energy flux from the warm side to the cold side

For two-state particles diffusing in a temperature gradient, the energy flux associated to transport of heat across the system is:

$$J_E = -E_1 D_1 \partial_x P_1 - E_2 D_2 \partial_x P_2 \tag{A.14}$$

where $-D_i\partial_x P_i$ is the diffusive probability flux for the state i. Writing P_1 and P_2 as functions of P_{tot} and Π, we have:

$$J_E = -\left(\frac{E_1 D_1 + E_2 D_2}{2}\right)\partial_x P_{tot} - \left(\frac{E_1 D_1 - E_2 D_2}{2}\right)\partial_x \Pi. \tag{A.15}$$

Reminding that, at steady state, $\Pi^{ss} = -P^{ss}_{tot}\mathcal{D}/\Delta$ (see the previous subsection), after some algebra, we have:

$$J_E = \frac{1}{\Delta}(E_1 - E_2)D_1 D_2 \partial_x P^{ss}_{tot} \tag{A.16}$$

Spelling out $\partial_x P^{ss}_{tot}$ by inverting equation (A.13), we finally have:

$$\frac{J_E}{-\partial_x T} = \frac{E_1 - E_2}{D_1 - D_2} D_1 D_2 \frac{\partial_T\langle D\rangle_{eq}}{\langle D\rangle_{eq}} P^{ss}_{tot} = D_1 D_2 \frac{E_1 - E_2}{D_1 - D_2} S_T P^{ss}_{tot}. \tag{A.17}$$

Appendix B. Soret coefficient in the fast-reaction limit

B.1. Discrete chemical space

Let us start from the reaction–diffusion system defined in the main text:

$$\partial_t P_i = D_i \partial_x^2 P_i + \sum_{j=1}^{n} k_{ij} P_j. \tag{B.1}$$

Let us suppose that chemical reactions are faster than diffusion. Starting from equation (B.1), we can employ a standard time-scale separation analysis. First, we explicit the time scale of reaction rate, $k_{ij} = \tilde{k}_{ij}/\epsilon$, with $\epsilon \ll 1$. Second, we propose a solution in the following form:

$$P_i(x,t) = P_i^{(0)}(x,t) + \epsilon P_i^{(1)}(x,t) + \mathcal{O}(\epsilon^2). \tag{B.2}$$

Plugging this expression into equation (B.1), and solving order by order, we find the following zeroth order equation:

$$\sum_{j=1}^{n} \tilde{k}_{ij} P_j^{(0)}(x) = 0. \tag{B.3}$$

This means that $P_i^{(0)}(x,t)$ can be written as:

$$P_i^{(0)}(x) = \frac{1}{Z} e^{-\frac{E_i}{k_B T(x)}} \pi(x,t) = P_i^{(eq)}(x)\pi(x,t) \tag{B.4}$$

where $T(x)$ is the local temperature at position x, $Z = \sum_i e^{-E_i/k_B T(x)}$ is the partition function. In other words, it is the product of the Boltzmann distribution in chemical space and a generic time-dependent function.

At first order, summing over all chemical states, the system satisfies:

$$\partial_t \pi(x,t) = \sum_{j=1}^{n} D_j \partial_x^2 \left(P_j^{(\mathrm{eq})}(x)\pi(x,t) \right). \tag{B.5}$$

Noting that $\pi(x,t) = \sum_j P_j^{(0)}(x) = P_{\mathrm{tot}}(x)$, up to the leading order in ε, from equation (B.5), we obtain:

$$\begin{aligned} S_{\mathrm{T}}^{\mathrm{ch}} &= \frac{\partial_T \langle D \rangle_{\mathrm{eq}}}{\langle D \rangle_{\mathrm{eq}}} \\ &= \frac{1}{\langle D \rangle_{\mathrm{eq}}} \partial_T \left(\frac{\sum_i D_i e^{-E_i/k_B T}}{Z} \right) \\ &= \frac{1}{\langle D \rangle_{\mathrm{eq}}} \frac{1}{Z^2 k_B T^2} \left(Z \sum_i D_i E_i e^{-E_i/k_B T} - \sum_i E_i e^{-E_i/k_B T} \sum_i D_i e^{-E_i/k_B T} \right) \\ &= \frac{\langle ED \rangle_{\mathrm{eq}} - \langle E \rangle_{\mathrm{eq}} \langle D \rangle_{\mathrm{eq}}}{\langle D \rangle_{\mathrm{eq}} k_B T^2} \\ &= \frac{\mathbf{Cov}_{\mathrm{eq}}(E,D)}{\langle D \rangle_{\mathrm{eq}} k_B T^2} \end{aligned} \tag{B.6}$$

with the equilibrium ensemble average defined as:

$$\langle D \rangle_{\mathrm{eq}} = \frac{1}{Z} \sum_i D_i e^{-\frac{E_i}{k_B T(x)}}. \tag{B.7}$$

Hence, the (chemical) Soret coefficient is the ensemble covariance of energies and diffusion coefficients. This provides some physical insights into the thermophoresis problem from an energetic perspective. If energy and diffusion coefficients are positively correlated, i.e. particles in high-energy states diffuse faster, then the Soret coefficient is positive, and the particles tend to move from the hot region to the cold region. The opposite motion happens when there is a negative correlation.

The energetic barriers in figure 1 are

$$\mathbf{B} = \begin{pmatrix} 0, & 1.26389, & 1.29478, & 1.08516, & 1.00019 \\ 1.26389, & 0, & 1.08848, & 1.15062, & 0.934777 \\ 1.29478, & 1.08848, & 0, & 1.17868, & 0.393306 \\ 1.08516, & 1.15062, & 1.17868, & 0, & 1.17527 \\ 1.00019, & 0.934777, & 0.393306, & 1.17527, & 0 \end{pmatrix}, \tag{B.8}$$

where the (i, j) element is the barrier from i to j. They have been drawn from a uniform distribution between 0 and 2, for the sake of simplicity.

B.2. Continuous chemical space

A system may experience a continuum of possible internal states, and the reaction-diffusion equation results as a coarse-grained description of transitions among local minima. When this approximation is not valid, the complete dynamics of the system can be captured by a Fokker–Planck equation, as introduced in the main text:

$$\partial_t P = \nabla_q \underbrace{\left(\frac{1}{\gamma_q} P \nabla_q U_q + \nabla_q (D_q P) \right)}_{-J_q} + \partial_x \underbrace{(\partial_x (D_x P))}_{-J_x}. \tag{B.9}$$

where $P \equiv P(x, q)$, is the probability distribution in the position-chemical space. We aim at investigating the fast reaction limit in this context, i.e. the flux acting on chemical space, $J_q \to \tilde{J}_q/\epsilon$, with $\epsilon \ll 1$, is much stronger than the one acting on real space, J_x. This condition is also equivalent to the following assumption:

$$\frac{D_x}{D_q} = \epsilon \ll 1 \qquad \gamma_q D_q = k_B T(x) \tag{B.10}$$

where the last equality corresponds to the Einstein relation. Guessing a solution of the following form:

$$P = P^{(0)} + \epsilon P^{(1)} + \mathcal{O}(\epsilon^2). \tag{B.11}$$

at the zeroth order, we have:

$$0 = -\partial_q^2 P^{(0)} - \frac{1}{k_B T(x)} \partial_q (P^{(0)} \partial_q U_q) \tag{B.12}$$

By solving this equation, we have:

$$P^{(0)}(x, q) = \mathcal{P}(x) \exp\left(-\frac{U_q}{k_B T(x)} \right). \tag{B.13}$$

where $\mathcal{P}(x)$ has to be determined by solving the first order equation, and the other factor is the equilibrium distribution in chemical space. At first order, integrating over the chemical space by employing the zero-flux condition, we have:

$$\partial_x^2 \left(\underbrace{\mathcal{P}(x) Z_q}_{\Phi(x)} \underbrace{\frac{1}{Z_q} \int_{-\infty}^{\infty} \mathrm{d}q \, \mathcal{P}(x) a(q) \exp\left(-\frac{U_q}{k_B T} \right)}_{D_{\mathrm{eff}}/\tilde{D}_x} \right) = 0, \tag{B.14}$$

where $P_{\mathrm{tot}}(x) = \int_d \mathrm{d}q \, P_0(x, q)$ is the marginal distribution along x, while the other term is the average of the D_x over chemical space. With an abuse of notation, we name P_{tot} the probability distribution integrated over the entire chemical space as the one in the discrete case, where a summation over internal states has been performed. Writing the ensemble average in chemical space as $\langle \cdot \rangle_q = \frac{1}{Z_q} \int_q \mathrm{d}q \, \cdot \exp\left(-\frac{U_q}{k_B T} \right)$, we obtain

$$\partial_x^2 (P_{\mathrm{tot}}(x) \langle D_x \rangle_q) = 0, \tag{B.15}$$

which is the same as the discrete-state case. The (chemical) Soret coefficient can be equally written in covariance form:

$$S_T^{\mathrm{ch}} = \frac{\partial_T \langle D_x \rangle_q}{\langle D_x \rangle_q} = \frac{\mathbf{Cov}_{\mathrm{eq}}(E, D_x)}{\langle D_x \rangle_{\mathrm{eq}} k_B T^2}. \tag{B.16}$$

In figure B2, we show that the stationary profile of P_{tot}, for a double well potential, exhibits a thermophoretic profile for three different choices of the diffusion coefficients.

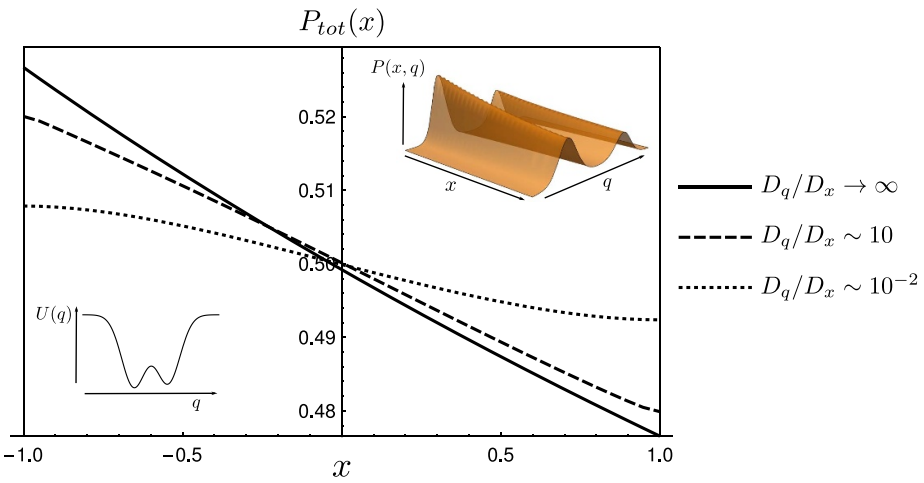


Figure B2. Stationary profile of the marginal distribution $P_{\rm tot}$, showing an accumulation of particles on the cold side of the gradient (on the left, in this case), for three different values of diffusion coefficients. *Upper inset*—Full distribution in the (x, q) space, with probability peaks corresponding to the location of wells in the subspace parametrized by q. *Lower inset*—The double-well potential is sketched. Here, we set the diffusion coefficients to $D(x) = 1$, and $D(q) = \alpha(U(q) + 2.5)$, where $\alpha = 10, 10^{-2}$ or $+\infty$, as indicated by the legend.

Appendix C. Smoluchowski equation from Kramers equation

C.1. Kramers equation and time-scales

Consider a particle with no internal (chemical) states. In the entire phase-space, it is described by the following Kramers equation:

$$\partial_t P(x,v,t) + v\partial_x P(x,v,t) = \frac{\gamma}{m}\partial_v\left(vP(x,v,t) + \frac{T(x)}{m}\partial_v P(x,v,t)\right). \tag{C.1}$$

For the sake of clarity, in this section we take $k_{\rm B} = 1$ in all the formulas presented. We assume that the system is operating in the overdamped regime, i.e. in a region of parameters where the time-scale associated to the friction, $\tau^{-1} = \gamma/m$ is much faster than all the others in play. It is then natural to employ a time-scale separation procedure to develop an equation describing the dynamics at the leading order.

In order to understand the correct scaling of equation (C.1) with respect to the expansion parameter $\tau \ll 1$, we perform the following change of variables:

$$\mathrm{x} = x\sqrt{\gamma} \qquad \mathrm{v} = v\sqrt{m}. \tag{C.2}$$

Then, in terms of these new variables, equation (C.1) becomes:

$$\tau\partial_t P(\mathrm{x},\mathrm{v},t) + \sqrt{\tau}\mathrm{v}\partial_{\mathrm{x}} P(\mathrm{x},\mathrm{v},t) = \partial_{\mathrm{v}}\left(\mathrm{v}P(\mathrm{x},\mathrm{v},t) + T(\mathrm{x})\partial_{\mathrm{v}} P(\mathrm{x},\mathrm{v},t)\right). \tag{C.3}$$

In the limit of small $1/\tau$, the probability distribution can be written as:

$$P(\mathrm{x},\mathrm{v},t) = P_0(\mathrm{x},\mathrm{v},t) + \sqrt{\tau}P_1(\mathrm{x},\mathrm{v},t) + \tau P_2(\mathrm{x},\mathrm{v},t) + \mathcal{O}\left(\tau^{3/2}\right) \tag{C.4}$$

since the smallest order appearing in the modified Kramers equation (C.3) is proportional to $\sqrt{\tau}$, which is then the natural expansion parameter to be adopted.

C.1.1. Zeroth order

Substituting equation (C.4) in equation (C.3) we obtain a set of equations at different orders in $\sqrt{\tau}$. The zeroth order equation is:

$$\partial_{\mathrm{v}}\left(\mathrm{v}P_0(\mathrm{x},\mathrm{v},t) + T(\mathrm{x})\partial_{\mathrm{v}} P_0(\mathrm{x},\mathrm{v},t)\right). \tag{C.5}$$

It is easy to verify that the solution is in the form $P_0(\mathrm{x},\mathrm{v},t) = e^{-\frac{\mathrm{v}^2}{2T(\mathrm{x})}}\Phi_0(\mathrm{x},t)$.

C.1.2. First order

The equation resulting from the first order terms is:

$$\mathrm{v}\partial_{\mathrm{x}}P_0(\mathrm{x},\mathrm{v},t) = \partial_{\mathrm{v}}\Big(\mathrm{v}P_1(\mathrm{x},\mathrm{v},t) + T(\mathrm{x})\partial_{\mathrm{v}}P_1(\mathrm{x},\mathrm{v},t)\Big) \tag{C.6}$$

Introducing the expression for P_0, and guessing the P_1 has a similar form, i.e. $P_1 = e^{-\frac{\mathrm{v}^2}{2T(\mathrm{x})}}\Phi_1(\mathrm{x},\mathrm{v},t)$, we get:

$$e^{-\frac{\mathrm{v}^2}{2T}}\Phi_0\frac{\mathrm{v}^3}{2T^2}\partial_{\mathrm{x}}T + \mathrm{v}e^{-\frac{\mathrm{v}^2}{2T}}\partial_{\mathrm{x}}\Phi_0 = \partial_{\mathrm{v}}\Big(\mathrm{v}P_1(\mathrm{x},\mathrm{v},t) + T\partial_{\mathrm{v}}P_1(\mathrm{x},\mathrm{v},t)\Big) = \partial_{\mathrm{v}}\Big(Te^{-\frac{\mathrm{v}^2}{2T}}\partial_{\mathrm{v}}\Phi_1\Big) \tag{C.7}$$

where, for sake of clarity, we have not reported all the dependence on x and v.

Guessing a solution of the form $\partial_{\mathrm{v}}\Phi_1(\mathrm{x},\mathrm{v},t) = -\partial_{\mathrm{x}}\Phi_0(\mathrm{x},t) + F_1(\mathrm{x},\mathrm{v},t)$, we obtain:

$$e^{-\frac{\mathrm{v}^2}{2T}}\Phi_0\frac{\mathrm{v}^3}{2T^2}\partial_{\mathrm{x}}T = \partial_{\mathrm{v}}\Big(Te^{-\frac{\mathrm{v}^2}{2T}}F_1\Big). \tag{C.8}$$

Integrating this equation between $-\infty$ and v', we get:

$$Te^{-\frac{\mathrm{v}'^2}{2T}}F_1 = -e^{-\frac{\mathrm{v}'^2}{2T}}\Phi_0\left(\mathrm{v}'^2 + 2T\right)\frac{1}{2T}\partial_{\mathrm{x}}T \to F_1 = -\frac{\mathrm{v}'^2 + 2T}{2T^2}\Phi_0\partial_{\mathrm{x}}T \tag{C.9}$$

where we assumed that the probability distribution has no divergent behavior at any order. Then, we have the following solution for the full probability distribution:

$$P(\mathrm{x},\mathrm{v},t) = e^{-\frac{\mathrm{v}^2}{2T}}\left\{\left(\Phi_0 + \sqrt{\tau}f(\mathrm{x},t)\right) - \sqrt{\tau}\left[\mathrm{v}\partial_{\mathrm{x}}\Phi_0 + \left(\frac{\mathrm{v}^3}{6T^2} + \frac{\mathrm{v}}{T}\right)\Phi_0\partial_{\mathrm{x}}T\right]\right\} + \mathcal{O}(\tau) \tag{C.10}$$

where $f(\mathrm{x},t)$ is an arbitrary function acting as a perturbation of $\Phi_0(\mathrm{x},t)$.

Moreover, $P(\mathrm{x},\mathrm{v},t)$ is the full probability distribution of x and v. However, we are interested in deriving an effective equation for the evolution of the marginal distribution of x and t. In fact, the time-scale expansion we have performed is compatible with the situation in which the variables v thermalize faster than x. Using the standard idea of the time-scale separation, we integrate over v, in order to understand what is the effective probability distribution we would like to describe, $\mathcal{P}(\mathrm{x},t)$, in terms of the full state space:

$$\mathcal{P}(\mathrm{x},t) = \int_{-\infty}^{+\infty}\mathrm{d}\mathrm{v}P(\mathrm{x},\mathrm{v},t) = \int_{-\infty}^{+\infty}\mathrm{d}\mathrm{v}e^{-\frac{\mathrm{v}^2}{2T(\mathrm{x})}}\Phi_0(\mathrm{x},t) = \Phi_0(\mathrm{x},t)\langle 1\rangle \tag{C.11}$$

where, from now on, we adopt the following notation: $\langle\cdot\rangle = \int_{-\infty}^{+\infty}\cdot\, e^{-\frac{\mathrm{v}^2}{2T(\mathrm{x})}}\mathrm{d}\mathrm{v}$. The integration can be easily performed by noting the parity of the function involved.

C.1.3. Second order

Going up to the second order in $\sqrt{\tau}$, and using the general expressions for P_0 and P_1, we obtain the following equation:

$$\partial_t\left(e^{-\frac{\mathrm{v}^2}{2T}}\Phi_0\right) + \mathrm{v}\partial_{\mathrm{x}}\left(e^{-\frac{\mathrm{v}^2}{2T}}\Phi_1\right) = \partial_{\mathrm{v}}\Big(\mathrm{v}P_2 + T\partial_{\mathrm{v}}P_2\Big). \tag{C.12}$$

Since we want to find the dynamical evolution of the function $\mathcal{P}(\mathrm{x},t) = \Phi_0(\mathrm{x},t)\langle 1\rangle$ defined in equation (C.11), we integrate equation (C.12) over the domain of v, obtaining:

$$\langle 1\rangle\partial_t\Phi_0(\mathrm{x},t) + \partial_{\mathrm{x}}\left(\langle\mathrm{v}\Phi_1(\mathrm{x},\mathrm{v},t)\rangle\right) = \partial_t\mathcal{P}(\mathrm{x},t) + \partial_{\mathrm{x}}\left(\langle\mathrm{v}\Phi_1(\mathrm{x},\mathrm{v},t)\rangle\right) = 0 \tag{C.13}$$

where we have used again the non-singularity condition of the probability distribution.

Here, we evaluate the following integral:

$$\langle\mathrm{v}\Phi_1(\mathrm{x},\mathrm{v},t)\rangle = -\langle\mathrm{v}^2\rangle\partial_{\mathrm{x}}\Phi_0 - \langle\mathrm{v}^4\rangle\frac{\Phi_0}{6T(\mathrm{x})^2}\partial_{\mathrm{x}}T(\mathrm{x}) - \langle\mathrm{v}^2\rangle\frac{\Phi_0}{T(\mathrm{x})}\partial_{\mathrm{x}}T(\mathrm{x}). \tag{C.14}$$

Notice that the function f introduced in equation (C.10) disappears after the integration over v both in the evaluation of $\mathcal{P}$, equation (C.11), and in the equation above. Then, f has no effect in the limit of thermalizing velocities (i.e. overdamped) we are considering.

Using the fact that $\langle \mathrm{v}^4 \rangle$ and $\langle \mathrm{v}^2 \rangle$ can be evaluated explicitly, and that the following relation holds: $\langle \mathrm{v}^4 \rangle = 3\langle \mathrm{v}^2 \rangle T(\mathrm{x})$, we get:

$$\langle \mathrm{v}\Phi_1(\mathrm{x},\mathrm{v},t)\rangle = -\langle \mathrm{v}^2\rangle \partial_\mathrm{x}\Phi_0 - \langle \mathrm{v}^2\rangle \frac{3\Phi_0}{2T(\mathrm{x})}\partial_\mathrm{x}T(\mathrm{x}). \tag{C.15}$$

Moreover, we highlight that:

$$\partial_x\langle \mathrm{v}^2\rangle = \langle \mathrm{v}^4\rangle \frac{\partial_\mathrm{x}T(\mathrm{x})}{2T(\mathrm{x})^2} = \langle \mathrm{v}^2\rangle \frac{3}{2}\frac{\partial_\mathrm{x}T(\mathrm{x})}{T(\mathrm{x})}. \tag{C.16}$$

Substituting this equality in equation (C.15), we finally get:

$$\langle \mathrm{v}\Phi_1(\mathrm{x},\mathrm{v},t)\rangle = -\langle \mathrm{v}^2\rangle \partial_\mathrm{x}\Phi_0(\mathrm{x},t) - \Phi_0(\mathrm{x},t)\partial_\mathrm{x}\langle \mathrm{v}^2\rangle = -\partial_\mathrm{x}\left(\langle \mathrm{v}^2\rangle \Phi_0(\mathrm{x},t)\right) \tag{C.17}$$

Then, equation (C.18), in terms of the marginal probability distribution $\mathcal{P}(\mathrm{x},t)$, becomes:

$$\partial_t\mathcal{P}(\mathrm{x},t) = \partial_\mathrm{x}\left[\partial_\mathrm{x}\left(\frac{\langle \mathrm{v}^2\rangle}{\langle 1\rangle}\mathcal{P}(\mathrm{x},t)\right)\right] = \partial_\mathrm{x}\left[\partial_\mathrm{x}\left(\langle \mathrm{v}^2\rangle_\mathrm{eq}\mathcal{P}(\mathrm{x},t)\right)\right] \tag{C.18}$$

which is the standard Smoluchowski equation, where $D(\mathrm{x}) = \langle \mathrm{v}^2\rangle_\mathrm{eq}$. Note that we identified $\langle \mathrm{v}^2\rangle/\langle 1\rangle = \langle \mathrm{v}^2\rangle_\mathrm{eq}$, that is the equilibrium ensemble average of v^2.

C.1.4. Conclusions

Hence, the origin of the thermophoretic effect for hard spheres, with no internal states, diffusing in a temperature gradient has to be found in the fact that spheres with different velocities have different transport properties. In other words, the ensemble of possible states in the velocity space plays the same role of the internal states of a molecule. It is important to note that the integration over the velocity states is crucial, since it allows us to associate to the same position x a plethora of states with different velocities: this is why these latter assume the same flavour of internal (e.g. configurational, energetic) states.

By writing down the expression of $D(\mathrm{x})$, and mapping back the final equation to the original variables (x, v), we obtain the following standard Smoluchowski equation with a diffusion coefficient satisfying Einstein relation, as for the original Kramers equation we started with:

$$\partial_t\mathcal{P}(x,t) = \frac{m}{\gamma}\partial_x^2\left(\langle v^2\rangle_\mathrm{eq}\mathcal{P}(x,t)\right) = \partial_x^2\left(D(x)\mathcal{P}(x,t)\right) \tag{C.19}$$

where $D(x) = T(x)/\gamma$ is the standard overdamped diffusion coefficient. The resulting Soret coefficient, S_T^0 in the main text, is exactly $1/T$.

C.1.5. Beyond the second order—determination of $f(x,t)$

The second order equation (C.12) can be solved by looking for a solution of the form $P_2 = e^{-\frac{\mathrm{v}^2}{2T(\mathrm{x})}}\Phi_2(\mathrm{x},\mathrm{v},t)$, and integrating over v' between $-\infty$ and v, as before. This leads to:

$$\langle 1\rangle^{(\mathrm{v})}\partial_t\Phi_0 + \partial_\mathrm{x}\langle \mathrm{v}\Phi_1\rangle^{(\mathrm{v})} = Te^{-\frac{\mathrm{v}^2}{2T}}\partial_\mathrm{v}\Phi_2 \tag{C.20}$$

employing the non-singular behavior of P_2, where $\langle\cdot\rangle^{(\mathrm{v})} = \int_{-\infty}^{\mathrm{v}}$. Expressing $\langle\cdot\rangle^{(v)}$ in terms of $\langle\cdot\rangle$, we obtain:

$$\langle 1\rangle^{(\mathrm{v})}\partial_t\Phi_0 + \partial_\mathrm{x}\langle \mathrm{v}\Phi_1\rangle^{(\mathrm{v})} = \frac{1}{2}\left(1 + erf\left(\frac{\mathrm{v}}{\sqrt{2T}}\right)\right)\left(\langle 1\rangle\partial_t\Phi_0 + \partial_x\langle \mathrm{v}\Phi_1\rangle\right) + e^{-\frac{\mathrm{v}^2}{2T}}I(\mathrm{x},\mathrm{v}) \tag{C.21}$$

where $I(\mathrm{x},\mathrm{v})$ is the remaining integral that does not contain exponential terms. Using the Smoluchowski equation, equation (C.18):

$$\partial_\mathrm{v}\Phi_2 = \frac{1}{T}I(\mathrm{x},\mathrm{v}). \tag{C.22}$$

Writing the third order equation, we get:

$$\partial_t P_1 + \mathrm{v}\partial_\mathrm{x}P_2 = \partial_\mathrm{v}\left(\mathrm{v}P_3 + \partial_\mathrm{v}P_3\right). \tag{C.23}$$

Integrating over v in the whole range of the velocities (from $-\infty$ to $+\infty$), we obtain:

$$\partial_t f = -\frac{1}{\langle 1\rangle}\partial_\mathrm{x}\left(T(\mathrm{x})\langle\partial_\mathrm{v}\Phi_2\rangle\right) = -\frac{1}{\langle 1\rangle}\partial_\mathrm{x}\langle I(\mathrm{x},\mathrm{v})\rangle. \tag{C.24}$$

Spelling out the integral, we have:

$$\partial_t f = T\partial_x^2 f + 3\partial_x T\partial_x f + 3f\frac{(\partial_x T)^2 + 2T\partial_x^2 T}{4T}. \tag{C.25}$$

If at $t = 0$, $f(\mathrm{x}, 0) = 0$, imposing an initial condition only on Φ_0 satisfying the Smoluchowski equation, then $f = 0$ at all times and x, consistently with the equation above.

C.2. Fluxes and velocity fronts

Let us study probability fluxes. The Kramers equation is a two-dimensional Fokker–Planck equation whose flux is a two-dimensional vector:

$$\partial_t P(\mathrm{x}, \mathrm{v}, t) = \begin{pmatrix} \partial_\mathrm{x} & \partial_\mathrm{v} \end{pmatrix} \begin{pmatrix} J_x \\ J_v \end{pmatrix} = \begin{pmatrix} \partial_x & \partial_v \end{pmatrix} \begin{pmatrix} \frac{1}{\sqrt{\gamma}} J_x \\ \frac{1}{\sqrt{m}} J_v \end{pmatrix} \tag{C.26}$$

writing the gradient in real space (x, v). Here, we have:

$$\begin{pmatrix} J_x \\ J_v \end{pmatrix} = \begin{pmatrix} -vP(x,v,t) \\ \frac{\gamma}{m}\left(vP(x,v,t) + \frac{T(x)}{m}\partial_v P(x,v,t)\right) \end{pmatrix} = \vec{J}. \tag{C.27}$$

Since velocity-space thermalizes much faster by assumption, we are interested in the position of particles. Thus, we will focus our attention only at the first component, J_x.

If we integrate J_x over the full velocity-space, by construction, we recover the standard flux of the Smoluchowski equation, J_S. Here, the second component J_v does not play a role since the limit of equilibrated velocities is implicitly considered.

$$J_\mathrm{S} = \frac{m}{\gamma}\partial_x\left(\frac{\langle v^2\rangle}{\langle 1\rangle}\mathcal{P}\right) = \langle \mathrm{v}\Phi_1\rangle = \int_{-\infty}^{+\infty} \mathrm{d}v J_x \tag{C.28}$$

where the first equality has been derived above for scaled variables, and the last one has been obtained using the parity of the functions involved. Here, we are considering the probability distribution up to the first order in $\sqrt{\tau}$. If we include the zero-flux boundary condition, at the stationary state, we have $J_\mathrm{S} = 0$, which is exactly the same condition we used to derive the Soret coefficient. Remembering that fast and slow particles have different transport properties, leading to the appearance of thermophoresis, for a system in the stationary state, we have:

$$J_\mathrm{slow} = \int_{-|v'|}^{|v'|} \mathrm{d}v J_x \qquad J_\mathrm{fast} = \int_{-\infty}^{-|v'|} \mathrm{d}v J_x + \int_{|v'|}^{+\infty} \mathrm{d}v J_x \qquad J_\mathrm{fast} = -J_\mathrm{slow} \tag{C.29}$$

since $J_\mathrm{fast} + J_\mathrm{slow} = J_\mathrm{S} = 0$. Then, hot and cold fluxes balance each other for any value of $|v'|$, in order to have a zero flux at the level of Smoluchowski equation. However, the system still preserves the presence of microscopic fluxes in the velocity space.

By developing the integral, using equation (C.11), and remembering that $S_\mathrm{T} = 1/T$ in this case, J_slow has the following expression:

$$J_\mathrm{slow} = \frac{\partial_x T}{\sqrt{2\pi T/m}}|v'|^3 e^{-\frac{m|v'|^2}{2T}}\mathcal{P} \propto \partial_x T. \tag{C.30}$$

Hence, J_slow is parallel to $\partial_x T$, while J_fast is parallel to $-\partial_x T$. Furthermore, J_slow is zero only at $|v'| \to 0$ and $|v'| \to \infty$, reaching a maximum at the critical velocity front $|v'| = v^*(x) = \sqrt{3T(x)/m}$.

C.3. Energy flux

The kinetic energy flux accounts for the amount of energy transported across the system. To show that our model is thermodynamically consistent, we show that:

$$J_x^E = \int_{-\infty}^{+\infty} \mathrm{d}v \frac{mv^2}{2} J_x = -\frac{D(x)}{2}\mathcal{P}\partial_x T \propto -\partial_x T. \tag{C.31}$$

This result has been obtained after some algebra, using equation (C.11), and the fact that $S_\mathrm{T} = 1/T$. The minus sign indicates that the energy flows from the warm to the cold side, as dictated by thermodynamics. At stationarity, $\mathcal{P}$ assumes it stationary value, and J_x^E becomes as the formula shown in the main text.

Appendix D. Soret coefficient for chemical reaction systems

Consider the fact that each chemical state has its own velocity distribution in the phase-space. Performing the overdamped limit, we already know that the resulting Fokker–Planck equation depends on a temperature modulated diffusion coefficient for each degree of freedom, $D_i(T)$. Thus, in the case of a discrete chemical space, we have:

$$\partial_t P_i = \partial_x^2 (D_i(T) P_i) + \sum_j k_{ij}(T) P_j. \tag{D.1}$$

Proceeding as before, in the fast reaction limit, we obtain the following steady-state equation for $P_{\rm tot} = \sum_i P_i$:

$$\partial_x \left(\langle D(T) \rangle_{\rm eq} P_{\rm tot} \right) = 0. \tag{D.2}$$

Hence, writing $D_i(T) = d_i T$, in accordance to the Stokes–Einstein relation and the derivation of the previous section, the corresponding Soret coefficient reads as follows:

$$S_{\rm T} = \frac{\partial_T \sum_i D_i(T) P_i^{(\rm eq)}}{\sum_i D_i(T) P_i^{(\rm eq)}} = \underbrace{\frac{\sum_i d_i \partial_T P_i^{(\rm eq)}}{\sum_i d_i P_i^{(\rm eq)}}}_{S_T^{\rm ch}} + \underbrace{\frac{\sum_i d_i P_i^{(\rm eq)}}{\sum_i d_i P_i^{(\rm eq)}} \frac{\partial_T T}{T}}_{S_{\rm T}^0} = S_{\rm T}^{\rm ch} + S_{\rm T}^0. \tag{D.3}$$

In the specific 2-state case presented in the main text, in which the transition rates contains also an additional entropic factor, we can compute the chemical Soret coefficient as follows:

$$\begin{aligned} S_{\rm T}^{\rm ch} &= \left(\frac{D_u (k_{f\to u}/k_{u\to f}) + D_f}{(k_{f\to u}/k_{u\to f}) + 1} \right)^{-1} \partial_T \left(\frac{D_u (k_{f\to u}/k_{u\to f}) + D_f}{(k_{f\to u}/k_{u\to f}) + 1} \right) \\ &= \frac{(R_d - 1) e^{\epsilon} \gamma \epsilon}{(e^{\epsilon} + \gamma)(e^{\epsilon} + R_d \gamma)} \frac{1}{T} \end{aligned}. \tag{D.4}$$

where we identified $d_u \equiv D_u$ and $d_f \equiv D_f$ for sake of simplicity, and employed the detailed balance relation $k_{f\to u}/k_{u\to f} = \gamma e^{-\epsilon}$, with $\epsilon = \varepsilon / k_{\rm B} T$ the rescaled energy difference. $S_{\rm T}^0 = 1/T$ by construction.

Appendix E. Soret coefficient and dimer formation

The system is described by the following reaction–diffusion equation (see main text):

$$\begin{aligned} \partial_t c_1 &= 2k_- c_2 - 2k_+ c_1^2 + D_1 \partial_x^2 c_1 \\ \partial_t c_2 &= k_+ c_1^2 - k_- c_2 + D_2 \partial_x^2 c_2 \end{aligned} \tag{E.1}$$

where c_1 and c_2 are, respectively, monomer and dimer concentrations, satisfying the normalization condition $c_1 + 2c_2 = c_{\rm tot}$, with $c_{\rm tot}$ total concentration. The dissociation constant has the usual form $K_d(x) = \frac{k_-(x)}{k_+(x)}$, where both association and dissociation rates depend on space through temperature.

Performing the fast reaction limit, the (chemical) Soret coefficient is defined by:

$$S_T \partial_x T = \frac{\partial_x \langle D \rangle_{\rm eq}}{\langle D \rangle_{\rm eq}} = -\frac{\partial_x c_{\rm tot}}{c_{\rm tot}} \tag{E.2}$$

where $\langle \cdot \rangle = c_{\rm tot}^{-1} \sum_{n=1}^{2} \cdot n c_n^{\rm eq}$, where n is the stoichiometric number, which is 1 for monomers, and 2 for dimers. Here, $c_n^{\rm eq}$ satisfies the chemical part of equation (E.1), resulting in the following expression:

$$c_1^{\rm eq} = c_{\rm tot} \frac{2}{1 + \sqrt{1 + 8(c_{\rm tot}/K_d)}} \qquad c_2^{\rm eq} = \frac{c_{\rm tot}}{2} \left(1 - c_1^{\rm eq} \right). \tag{E.3}$$

We remind that $c_{\rm tot}$ and K_d depend on space, thus also $c_1^{\rm eq}$ and $c_2^{\rm eq}$ do. Let us evaluate the expression of $\partial_x \langle D \rangle_{\rm eq}$:

$$\begin{aligned} \partial_x \langle D \rangle_{\rm eq} = \partial_x \left(\frac{D_1 c_1^{\rm eq} + 2 D_2 c_2^{\rm eq}}{c_{\rm tot}} \right) &= (D_1 - D_2) \partial_x \left(\frac{c_1^{\rm eq}}{c_{\rm tot}} \right) \\ &= (D_1 - D_2) \frac{(c_1^{\rm eq}/c_{\rm tot})^2}{\sqrt{1 + 8(c_{\rm tot}/K_d)}} \partial_x \left(\frac{c_{\rm tot}}{K_d} \right) \end{aligned}. \tag{E.4}$$

By inverting the last equality of equation (E.2), we have:

$$\begin{aligned}\partial_x c_{\rm tot} &= c_{\rm tot}(D_1 - D_2)\frac{(c_1^{\rm eq}/c_{\rm tot})^2}{\sqrt{1+8(c_{\rm tot}/K_d)}}\partial_x\left(\frac{c_{\rm tot}}{K_d}\right)\frac{1}{\langle D\rangle_{\rm eq}} \\ &= \frac{D_1 - D_2}{\langle D\rangle_{\rm eq}} g(T, K_d, c_{\rm tot})\partial_x\left(\frac{c_{\rm tot}}{K_d}\right)\end{aligned} \tag{E.5}$$

where g is a positive function. Naming $g(D_1 - D_2)/\langle D\rangle_{\rm eq} \equiv F$, and recalling that $D_1 > D_2$ in this case, we have that also F is a positive function. Hence, solving equation (E.5) for $\partial_x c_{\rm tot}$, we have:

$$\partial_x c_{\rm tot} = -\frac{F c_{\rm tot}}{1 - K_d F}\partial_x K_d. \tag{E.6}$$

Putting equation (E.6) back into equation (E.2), we have the expression for the (chemical) Soret coefficient shown in the main text:

$$S_{\rm T} = \frac{F}{1 - K_d F}\partial_T K_d \tag{E.7}$$

ORCID iDs

Shiling Liang (梁师翎) https://orcid.org/0000-0001-8968-8443
Daniel Maria Busiello https://orcid.org/0000-0002-6754-5019

References

[1] Rahman M and Saghir M 2014 Thermodiffusion or Soret effect: historical review *Int. J. Heat Mass Transfer* **73** 693–705
[2] Platten. J K 2005 The Soret effect: a review of recent experimental results *J. Appl. Mech.* **73** 5–15
[3] Piazza R 2008 Thermophoresis: moving particles with thermal gradients *Soft Matter* **4** 1740–4
[4] Ludwig C 1856 Diffusion zwischen ungleich erwärmten Orten gleich zusammengesetzter Lösungen : Sitzung vom 8. Mai 1856 *Sitzungsberichte der mathematisch-naturwissenschaftlichen Classe der Kaiserlichen Akademie der Wissenschaften Wien* vol 3 (Wien: K.K. Hof- und Staatsdruckerei) p 539
[5] Iacopini S, Rusconi R and Piazza R 2006 The 'macromolecular tourist': universal temperature dependence of thermal diffusion in aqueous colloidal suspensions *Eur. Phys. J.* E **19** 59–67
[6] Iacopini S and Piazza R 2003 Thermophoresis in protein solutions *EPL (Europhys. Lett.)* **63** 247
[7] Niether D and Wiegand S 2019 Thermophoresis of biological and biocompatible compounds in aqueous solution *J. Phys.: Condens. Matter* **31** 503003
[8] Köhler W and Morozov K I 2016 The Soret effect in liquid mixtures–a review *J. Non-Equilib. Thermodyn.* **41** 151–97
[9] Duhr S, Arduini S and Braun D 2004 Thermophoresis of DNA determined by microfluidic fluorescence *Eur. Phys. J.* E **15** 277–86
[10] Piazza R and Parola A 2008 Thermophoresis in colloidal suspensions *J. Phys.: Condens. Matter* **20** 153102
[11] Würger A 2010 Thermal non-equilibrium transport in colloids *Rep. Prog. Phys.* **73** 126601
[12] Würger A 2013 Is Soret equilibrium a non-equilibrium effect? *C. R. - Mec.* **341** 438–48
[13] Soret C 1879 Etat d'équilibre des dissolutions dont deux parties sont portées à des températures différentes *Arch. Sci. Phys. Nat. Geneve* **2** 48–64
[14] See appendix for analytical derivations and mathematical details
[15] Burelbach Jerôme, Frenkel D, Pagonabarraga I and Eiser E 2018 A unified description of colloidal thermophoresis *Eur. Phys. J.* E **41** 1–12
[16] Duhr S and Braun D 2006 Why molecules move along a temperature gradient *Proc. Natl Acad. Sci.* **103** 19678–82
[17] Duhr S and Braun D 2006 Thermophoretic depletion follows Boltzmann distribution *Phys. Rev. Lett.* **96** 168301
[18] Kita R and Wiegand S 2005 Soret coefficient of poly (n-isopropylacrylamide)/water in the vicinity of coil- globule transition temperature *Macromolecules* **38** 4554–6
[19] Wongsuwarn S, Vigolo D, Cerbino R, Howe A M, Vailati A, Piazza R and Cicuta P 2012 Giant thermophoresis of poly(n-isopropylacrylamide) microgel particles *Soft Matter* **8** 5857–63
[20] Königer A, Plack N, Köhler W, Siebenbürger M and Ballauff M 2013 Thermophoresis of thermoresponsive polystyrene–poly (n-isopropylacrylamide) core–shell particles *Soft Matter* **9** 1418–21
[21] Maeda Y T, Tlusty T and Libchaber A 2012 Effects of long DNA folding and small RNA stem–loop in thermophoresis *Proc. Natl Acad. Sci.* **109** 17972–7
[22] Würger A 2014 Do thermal diffusion and Dufour coefficients satisfy onsager's reciprocity relation? *Eur. Phys. J.* E **37** 1–11
[23] Ham. J S 1960 Kinetic theory of thermal diffusion in dilute polymer solutions *J. Appl. Phys.* **31** 1853–8
[24] Busiello D M, Liang S, Piazza F and De Los Rios P 2021 Dissipation-driven selection of states in non-equilibrium chemical networks *Commun. Chem.* **4** 1–7
[25] Busiello D M, Gupta D and Maritan A 2020 Coarse-grained entropy production with multiple reservoirs: unraveling the role of time scales and detailed balance in biology-inspired systems *Phys. Rev. Res.* **2** 043257
[26] Dass A V, Georgelin T, Westall F, Foucher F, De Los Rios P, Busiello D M, Liang S and Piazza F 2021 Equilibrium and non-equilibrium furanose selection in the ribose isomerisation network *Nat. Commun.* **12** 1–10
[27] Calvin Giddings J 1993 Field-flow fractionation: analysis of macromolecular, colloidal and particulate materials *Science* **260** 1456–65
[28] Geelhoed P F, Lindken R and Westerweel J 2006 Thermophoretic separation in microfluidics *Chem. Eng. Res. Des.* **84** 370–3

[29] Sekimoto K 1999 Temporal coarse graining for systems of Brownian particles with non-constant temperature *J. Phys. Soc. Japan* **68** 1448–9
[30] Matsuo M and Sasa S-ichi 2000 Stochastic energetics of non-uniform temperature systems *Physica A* **276** 188–200
[31] Lau A W C and Lubensky T C 2007 State-dependent diffusion: thermodynamic consistency and its path integral formulation *Phys. Rev.* E **76** 011123
[32] Kupferman R, Pavliotis G A and Stuart A M 2004 Itô versus stratonovich white-noise limits for systems with inertia and colored multiplicative noise *Phys. Rev.* E **70** 036120
[33] Graham R and Schenzle A 1982 Stabilization by multiplicative noise *Phys. Rev.* A **26** 1676
[34] Reichl M, Herzog M, Götz A and Braun D 2014 Why charged molecules move across a temperature gradient: The role of electric fields *Phys. Rev. Lett.* **112** 198101
[35] Wang Z, Kriegs H and Wiegand S 2012 Thermal diffusion of nucleotides *J. Phys. Chem.* B **116** 7463–9
[36] Mohanakumar S, Luettmer-Strathmann J and Wiegand S 2021 Thermodiffusion of aqueous solutions of various potassium salts *J. Chem. Phys.* **154** 084506